ISTS-2017-d-118／ISSFD-2017-118

Attitude and Orbit Coupled Tumbling Space Debris Tracking Control

By Shuquan WANG,[1)] Lingchao ZHU,[1),2)]

[1)] *Technology and Engineering Center for Space Utilization, China Academy of Sciences, Beijing, China*
[2)] *University of Chinese Academy of Sciences, Beijing, China*

(Received April 17th, 2017)

The tracking control of rotating space debris is investigated in this paper. The objective is to keep the tracking spacecraft stay at a certain distance above the specific face of the space debris, while the spacecraft's certain instrument should point to the space debris during the process. The expected motion of the tracking spacecraft is determined by the space debris's orbital and attitude status and the relative motion between the two bodies. A highly coupled control strategy, with the awareness of the singularity rejection, is developed to fulfill the tracking mission. Numerical simulations demonstrate the effectiveness of the tracking control.

Key Words: Space Debris, Formation Flying, Nonlinear Control.

1. Introduction

The number of space debris has increased rapidly in recent years, which causes a serious space security problem. In the near-Earth orbit, the probability of collision between satellite and space debris would grow with the increase of space debris, a chain reaction caused by the collision will further increase the amount of space debris. For those reason, the study of space debris cleanup is important. The mainly methods of space debris cleanup methods divided into passive,[1)] active[2)] and hybrid cleaning methods.[3)] Active cleaning methods include the thrust deorbit method, the manipulator capture method, expandable foam method, where the manipulator capture method comprises three parts, the motion observation of space debris, the motion control of tracking spacecraft and the motion control of manipulator respectively.

There is growing concern over orbital tracking and space debris cleaning. T Schildknecht reviewed the results from optical surveys for space debris in high-altitude Earth orbits and predicted the influence of space debris on the future of space research and space astronomy.[4)] The feasibility study of a mission in which the debris is removed by using a hybrid propulsion module as propulsion unit was presented by L.T. DeLuca.[5)] A new brush type contactor as end-effecter of a robot arm was proposed for a removal work strategy and control method for capturing and braking a tumbling, non-cooperative target space debris.[6)] The target spacecraft real-time tracking problems under the condition of the gravity field were presented by Estabrook.[7)] A Lyapunov-based, nonlinear, adaptive control law was developed by Marcio S for the problem of relative position control for multiple spacecraft.[8)] Bo J N applied generic control strategies to solve the problem of maintaining and maneuvering a formation of Earth observing satellites, which considered several constraints including fixed thrust magnitude and non-radial thrusting.[9)] An adaptive finite-time control for spacecraft hovering over an asteroid was presented by Lee D, an adaptive FTSMC scheme was proposed which does not require a priori knowledge of the uncertainties and disturbance bounds.[10)] A teardrop hovering formation is obtained and a new impulsive control strategy is proposed to keep the chasing satellite in the hovering pattern for a long term by Rao Y.[11)] Thein M W[12)] did research of a minimum configuration and developed an algorithm to estimate the relative position of two spacecraft by using a sliding mode observer.

As for attitude tracking problems, extensive studies have been conducted. A geometric method on the two-sphere was proposed by Ramp M for attitude and angular velocity tracking for a rigid body,[13)] a new attitude error function was constructed to avoid unwinding or singularities problems. A new class of angular velocity-free attitude stabilization controllers was designed by Subbarao K,[14)] it were generalizations of the passivity-based control algorithms. A global set stabilization method for the attitude control based on quaternion was developed by Li S,[15)] a finite-time control law was designed which can force spacecraft's angular velocity to track the virtual optimal angular velocity in finite time. a hybrid PID attitude control law was developed by Su J[16)] which was robust to external constant disturbance torques and measurement noise. Wisniewski R developed linear attitude control strategies for a low earth orbit small satellite actuated by electromagnetic coils and an excellent frame for investigations was given by a solution of the Riccati equation.[17)] A fault tolerant attitude tracking control scheme was developed in the face of faulty actuator, system uncertainties, external disturbances and actuator saturation by Xiao B,[18)] an adaptive sliding mode controller was derived and a modified fault tolerant control law was presented to address actuator saturation problem. A finite-time attitude tracking control scheme was proposed by Zou A M for spacecraft using terminal sliding mode and Chebyshev neural network.[19)] A terminal sliding manifold was proposed for attitude tracking in the presence of an unknown mass moment of inertia matrix, disturbances, and control input constraints. For attitude control for large-angle slew maneuvers problem, Xing G Q[20)] used relative attitude kinematics and dynamics equations to construct Lyapunov attitude state tracking control law. Optimal adaptive controllers were designed for addressing attitude tracking control problem of a rigid spacecraft with external disturbances and an uncertain inertia matrix by Luo W,[21)] which was not only inverse optimal but also formed a closed-loop attitude system.

Extensive studies have been conducted about spacecraft's tracking problems with orbit-attitude coupling dynamics. Relative motion and attitude-orbit coupling formation flying and

adaptive tracking control law were given by Haizhou Pan.[22] An optimal controller for space debris's tracking using the $\theta - D$ method was presented by Xin.[23] Wu[24] designed a variable structure tracking controller to optimize thrust vector in formation spacecraft tracking control. Wang and Wu etc.[25] adopted dual quaternions to describe the relative motion with six degrees of freedom, model neutral PD control and adaptive variable structure controller with input saturation were considered to achieve attitude-orbit coupling control in the final stage of the rendezvous and docking. A guidance and a control law was developed to maneuver the boresight axis of a spacecraft relative to a reference vector by Pong C M which was practicable for pointing, attitude tracking, and searching.[26] Optimal control techniques was proposed for proximity operations and docking by Lee D R,[27] he developed two candidate controllers for translational motion and a linear quadratic Gaussian controller for precision attitude maneuvering.

When tracking spacecraft approach space debris close enough for manipulator's mission according to desired trajectory, the manipulator would recover or clean up space debris. Space debris's tracking is precondition of the manipulator capture method, this paper focuses on the space debris's tracking whose desired trajectory is determined by the space debris's orbital and attitude status. In the process of close-proximity tracking (Ten meters level), the objective is to keep the tracking spacecraft approach space debris along a surface normal direction and points to the specific face of the space debris, tracking spacecraft's desired relative position changes with the attitude of space debris.

These methods achieved satisfactory results in convergence rate, control precision, energy optimization etc. of relative motion control with six degrees of freedom. However, rotating space debris's tracking was not considered in these references. The tracking problem of rotating space debris is investigated in this paper. Calculation of the desired trajectory, tracking control algorithm, the stability analysis problem and other issues need to be resolved specifically. Keep the tracking spacecraft's barycenter track the specific face of the space debris is focus in this paper as the preliminary study of rotating space debris's tracking, the objective of tracking is to keep the tracking spacecraft stay at a certain distance above the surface normal direction of the space debris. The desired position of the tracking spacecraft's barycenter is determined by the relative orbital motion of the spacecraft relative to space debris and space debris's attitude status. Relative motion equation and the quaternions are utilized to describe the center of mass motion and the attitude motion respectively. A Lyapunov based nonlinear controller is developed to fulfill the tracking mission and stability analysis is given in this paper.

2. Equations of Motion

Assuming that the states of the translation motion and the attitude motion of a space debris are known, this paper investigates the close-proximity tracking of the space debris. A spacecraft is deployed to approach the space debris with an observing instrument (such as a camera) pointing towards a characteristic face of the space debris. The scenario is shown in Fig. 1. Because the space debris does not have maneuverability, in describing the relative motion the space debris is taken as the chief and the spacecraft is taken as deputy. The Hill frame is centered at the chief.

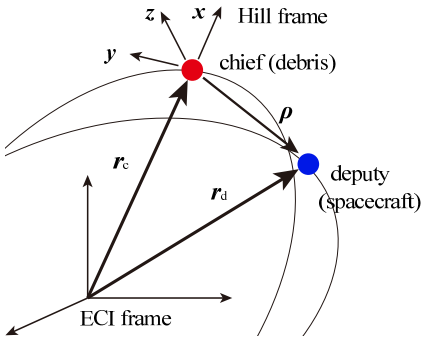

Fig. 1. Scenario of the two-object orbiting system.

The relative position of the deputy with respect to (w.r.t.) the chief is defined as

$$\boldsymbol{\rho} = \boldsymbol{r}_d - \boldsymbol{r}_c = {}^{H}[x, y, z]^T \tag{1}$$

where $\boldsymbol{R}_d$ and $\boldsymbol{R}_c$ are the position vectors of the deputy and the chief respectively w.r.t. the center of the Earth, ${}^{H}[x, y, z]^T$ represents the coordinates of the deputy in the Hill frame. The dynamics of the spacecraft and the space debris are

$$\ddot{\boldsymbol{r}}_d = -\frac{\mu}{r_d^3}\boldsymbol{r}_d + \boldsymbol{u} \tag{2}$$

$$\ddot{\boldsymbol{r}}_c = -\frac{\mu}{r_c^3}\boldsymbol{r}_c \tag{3}$$

where $r_c = \|\boldsymbol{R}_c\|$, $r_d = \|\boldsymbol{R}_d\|$, $\boldsymbol{u}$ is the control force acting on the spacecraft. The dynamics of the relative motion is given by[28]

$$\ddot{x} - 2\dot{f}\left(\dot{y} - y\frac{\dot{r}_c}{r_c}\right) - x\dot{f}^2 - \frac{\mu}{r_c^2} = -\frac{\mu}{r_d^3}(r_c + x) + u_x \tag{4a}$$

$$\ddot{y} + 2\dot{f}\left(\dot{x} - x\frac{\dot{r}_c}{r_c}\right) - y\dot{f}^2 = -\frac{\mu}{r_d^3}y + u_y \tag{4b}$$

$$\ddot{z} = -\frac{\mu}{r_d^3}z + u_z \tag{4c}$$

where f is the true anomaly angle of the chief, $\mu = 3.986 \times 10^{14}\mathrm{m}^3/\mathrm{s}^2$ is the Earth's gravitational coefficient, $[u_x, u_y, u_z]^T$ is the acceleration of the deputy projected in the Hill frame.

3. Baseline Position Tracking Control

This section tries to develop a controller such that the position of the spacecraft tracks the characteristic face of the space debris. To be more specifically, the expected location of the spacecraft is at a certain distance above the characteristic face of the space debris. Without loss of generality, it is assumed that the normal direction of the characteristic face of the space debris is the z axis of the space debris's body fixed frame. The objective is formulated as

$$\boldsymbol{\rho}_e = {}^{B}[0, 0, l_e]^T, \ \frac{{}^{B}\mathrm{d}\boldsymbol{\rho}_e}{\mathrm{d}t} = \boldsymbol{0}, \ \frac{{}^{B}\mathrm{d}^2\boldsymbol{\rho}_e}{\mathrm{d}t^2} = \boldsymbol{0} \tag{5}$$

where l_e is the expected distance between the spacecraft and the space debris. Note that as shown in Eq. (5), $\boldsymbol{\rho}_e$ is expressed in $\{\mathcal{B}\}$ frame, the derivative $\frac{{}^{B}\mathrm{d}\boldsymbol{\rho}_e}{\mathrm{d}t}$ is taken with respect to $\{\mathcal{B}\}$

frame. In developing the control algorithm, it is usually expected to use the desired states in the inertial frame or in the Hill frame. This paper chooses to develop the control algorithm in the inertial frame.

By the transport theorem, we have

$$\begin{aligned}\dot{\boldsymbol{\rho}} &= \frac{{}^{N}\mathrm{d}\boldsymbol{\rho}}{\mathrm{d}t} = \frac{{}^{B}\mathrm{d}\boldsymbol{\rho}}{\mathrm{d}t} + \boldsymbol{\omega}_{B/N} \times \boldsymbol{\rho} \\ \ddot{\boldsymbol{\rho}} &= \frac{{}^{N}\mathrm{d}^2\boldsymbol{\rho}}{\mathrm{d}t^2} = \frac{{}^{B}\mathrm{d}^2\boldsymbol{\rho}}{\mathrm{d}t^2} + 2\boldsymbol{\omega}_{B/N} \times \frac{{}^{B}\mathrm{d}\boldsymbol{\rho}}{\mathrm{d}t} \\ &\quad + \dot{\boldsymbol{\omega}}_{B/N} \times \boldsymbol{\rho} + \boldsymbol{\omega}_{B/N} \times (\boldsymbol{\omega}_{B/N} \times \boldsymbol{\rho}) \end{aligned} \tag{6}$$

where $\boldsymbol{\omega}_{B/N}$ is the angular velocity of the $\{\mathcal{B}\}$ frame w.r.t. the inertial frame. Substituting Eq. (5) into Eq. (6), yields

$$\dot{\boldsymbol{\rho}}_e = \boldsymbol{\omega}_{B/N} \times \boldsymbol{\rho}_e \tag{7a}$$

$$\ddot{\boldsymbol{\rho}}_e = \dot{\boldsymbol{\omega}}_{B/N} \times \boldsymbol{\rho}_e + \boldsymbol{\omega}_{B/N} \times (\boldsymbol{\omega}_{B/N} \times \boldsymbol{\rho}_e) \tag{7b}$$

Note that the expressions of the equations in Eq. (7) become very concise if the vectors are projected into the $\{\mathcal{B}\}$ frame.

Expected position in coordinate system $\{\mathcal{H}\}$ can be expressed as

$${}^{H}\boldsymbol{\rho}_e = Q_{HN} \cdot {}^{N}\boldsymbol{\rho}_e \tag{8}$$

where Q_{HN} is the coordinate-transformation matrix from the inertial frame to the $\{\mathcal{H}\}$ frame, and it can be expressed as

$$Q_{HN} = [\boldsymbol{i}, \boldsymbol{j}, \boldsymbol{k}]^T = \left[\frac{\boldsymbol{r}}{\| \boldsymbol{r} \|}, \boldsymbol{k} \times \boldsymbol{i}, \frac{\boldsymbol{r} \times \dot{\boldsymbol{r}}}{\| \boldsymbol{r} \times \dot{\boldsymbol{r}} \|}\right]^T \tag{9}$$

Then expected velocity in coordinate system $\{\mathcal{H}\}$ can be expressed as

$${}^{H}\dot{\boldsymbol{\rho}}_e = Q_{HN} \cdot A^T \cdot ({}^{B}\boldsymbol{\omega}_{B/N} \times {}^{B}\boldsymbol{\rho}_e) - {}^{H}\boldsymbol{\omega}_{H/N} \times {}^{H}\boldsymbol{\rho}_e \tag{10}$$

where A is the direction cosine matrix from the $\{\mathcal{B}\}$ frame to the inertial frame. Take the derivative of Eq. (10), yields

$$\begin{aligned}{}^{H}\ddot{\boldsymbol{\rho}}_e = \; & Q_{HN} \cdot A^T \left[{}^{B}\dot{\boldsymbol{\omega}}_{B/N} \times {}^{B}\boldsymbol{\rho}_e + {}^{B}\boldsymbol{\omega}_{B/N} \times ({}^{B}\boldsymbol{\omega}_{B/N} \times {}^{B}\boldsymbol{\rho}_e)\right] \\ & - 2{}^{H}\boldsymbol{\omega}_{H/N} \times {}^{H}\dot{\boldsymbol{\rho}}_e - {}^{H}\dot{\boldsymbol{\omega}}_{H/N} \times {}^{H}\boldsymbol{\rho}_e \\ & - {}^{H}\boldsymbol{\omega}_{H/N} \times ({}^{H}\boldsymbol{\omega}_{H/N} \times {}^{H}\boldsymbol{\rho}_e) \end{aligned} \tag{11}$$

Thus the expected position, velocity and acceleration of the spacecraft are

$$\boldsymbol{r}_{d,e} = \boldsymbol{r}_c + \boldsymbol{\rho}_e \tag{12a}$$

$$\dot{\boldsymbol{r}}_{d,e} = \dot{\boldsymbol{r}}_c + \dot{\boldsymbol{\rho}}_e \tag{12b}$$

$$\ddot{\boldsymbol{r}}_{d,e} = \ddot{\boldsymbol{r}}_c + \ddot{\boldsymbol{\rho}}_e \tag{12c}$$

Next the controller that drives the spacecraft follow the expected motion is to be developed. Define the tracking error in the $\{\mathcal{H}\}$ frame as

$$\Delta\boldsymbol{\rho} = \boldsymbol{\rho} - \boldsymbol{\rho}_e \tag{13}$$

Define a Lyapunov function as

$$V_1(\Delta\boldsymbol{\rho}, \Delta\dot{\boldsymbol{\rho}}) = \frac{1}{2}\Delta\boldsymbol{\rho}^T[K_1]\Delta\boldsymbol{\rho} + \frac{1}{2}\Delta\dot{\boldsymbol{\rho}}^T\Delta\dot{\boldsymbol{\rho}} \tag{14}$$

where $[K_1] \in \mathbb{R}^{3\times3}$ is a positive definite matrix. Taking a first order time derivative of Eq. (14), yields

$$\dot{V}_1 = \Delta\dot{\boldsymbol{\rho}}^T (\Delta\ddot{\boldsymbol{\rho}} + [K_1]\Delta\boldsymbol{\rho}) \tag{15}$$

where $\ddot{\boldsymbol{\rho}} = [\ddot{x}, \ddot{y}, \ddot{z}]$ can be solved by Eq. (4), abbreviate it as $\ddot{\boldsymbol{\rho}} = f(\boldsymbol{\rho}, \dot{\boldsymbol{\rho}}) + \boldsymbol{U}_H$.

Substituting Eqs. (4) into Eq. (15), yields

$$\dot{V}_1 = \Delta\dot{\boldsymbol{\rho}}^T (f(\boldsymbol{\rho}, \dot{\boldsymbol{\rho}}) - \ddot{\boldsymbol{\rho}}_e + \boldsymbol{U}_H + [K_1]\Delta\boldsymbol{\rho}) \tag{16}$$

Letting $\dot{V}_1$ to be negative semi definite:

$$\dot{V}_1 = -\Delta\dot{\boldsymbol{\rho}}^T[K_2]\Delta\dot{\boldsymbol{\rho}} \tag{17}$$

where $[K_2] \in \mathbb{R}^{3\times3}$ is positive definite. Substituting Eq. (11) and Eq. (17) into Eq. (16), yields the baseline translational controller

$$\begin{aligned}\boldsymbol{U}_H = & - f(\boldsymbol{\rho}, \dot{\boldsymbol{\rho}}) - [K_1]\Delta\boldsymbol{\rho} - [K_2]\Delta\dot{\boldsymbol{\rho}} \\ & + Q_{HN} \cdot A^T \left[{}^{B}\dot{\boldsymbol{\omega}}_{B/N} \times {}^{B}\boldsymbol{\rho}_e + {}^{B}\boldsymbol{\omega}_{B/N} \times ({}^{B}\boldsymbol{\omega}_{B/N} \times {}^{B}\boldsymbol{\rho}_e)\right] \\ & - 2{}^{H}\boldsymbol{\omega}_{H/N} \times {}^{H}\dot{\boldsymbol{\rho}}_e - {}^{H}\dot{\boldsymbol{\omega}}_{H/N} \times {}^{H}\boldsymbol{\rho}_e \\ & - {}^{H}\boldsymbol{\omega}_{H/N} \times ({}^{H}\boldsymbol{\omega}_{H/N} \times {}^{H}\boldsymbol{\rho}_e) \end{aligned} \tag{18}$$

Note that the control algorithm in Eq. (18) makes $\dot{V}_1$ satisfy Eq. (16). The expression in Eq. (16) is negative semi definite even though $[K_2]$ is positive definite. This is because of that the definition of V_1 in Eq. (14) is a function of $\Delta\boldsymbol{\rho}$ and $\Delta\dot{\boldsymbol{\rho}}$, while $\dot{V}_1$ is a function of only $\Delta\dot{\boldsymbol{\rho}}$. So far it is assured that the controller in Eq. (18) drives $\Delta\dot{\boldsymbol{\rho}}$ to zero and the system is stable. Whether or not $\Delta\boldsymbol{\rho}$ converges to zero needs more investigation.

Taking a first order time derivative of Eq. (17) and evaluate at $\Delta\dot{\boldsymbol{\rho}} = 0$, yields

$$\ddot{V}_1\Big|_{\Delta\dot{\boldsymbol{\rho}}=0} = 0 \tag{19}$$

Taking a second order time derivative of Eq. (17) and evaluate at $\Delta\dot{\boldsymbol{\rho}} = 0$, yields

$$\dddot{V}_1\Big|_{\Delta\dot{\boldsymbol{\rho}}=0} = -\Delta\boldsymbol{\rho}^T[K_1]^T[K_2][K_1]\Delta\boldsymbol{\rho} < 0 \tag{20}$$

Because the first nonzero derivative of V_1 is the third order derivative, and $\dddot{V}_1$ is a negative definite function of $\Delta\boldsymbol{r}$, it can be assured that $\Delta\boldsymbol{r}$ converges to zero as well. So the controller in Eq. (18) is asymptotically stable.

The control algorithm in Eq. (18) is a baseline position tracking control that drives the spacecraft to the expected trajectory. The phrase "baseline" means that Eq. (18) is not the final position tracking control. When the algorithm in Eq. (18) cooperates with the attitude controller that will be developed in the next section, a certain singularity issue arises. So the control algorithm in Eq. (18) needs to be modified. This issue will be discussed later on.

4. Attitude Pointing Control

The objective of the attitude control is to make a certain instrument, such as a Lidar or a camera, on the spacecraft to point towards the space debris, such that the spacecraft is able to measure the relative motion between the spacecraft and the space debris. Without loss of generality, this paper assumes that the z axis of the spacecraft's body frame should point to the space debris. The scenario is shown in Fig. 2.

The quaternions $\boldsymbol{q} = q_0 + \boldsymbol{i}q_1 + \boldsymbol{j}q_2 + \boldsymbol{k}q_3 = q_0 + \boldsymbol{q}_v$ are utilized to describe the attitude of the spacecraft and the space debris. The attitude kinematic and dynamic equations are as follows

$$\dot{\boldsymbol{q}} = \frac{1}{2}B(\boldsymbol{q})\,\boldsymbol{\omega} \tag{21}$$

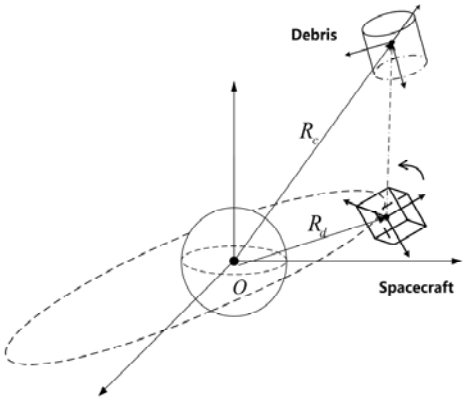

Fig. 2. Scenario of the orbital and attitude tracking.

$$\boldsymbol{J}\dot{\boldsymbol{\omega}} = -\boldsymbol{\omega} \times \boldsymbol{J}\boldsymbol{\omega} + \boldsymbol{T}_c \tag{22}$$

where $\boldsymbol{\omega}$ is the angular velocity of the spacecraft, $\boldsymbol{J}$ is the inertia matrix, $\boldsymbol{T}_c$ is the control torque, The operator $B(\boldsymbol{q})$ is given by

$$B(\boldsymbol{q}) = \begin{bmatrix} -\boldsymbol{q}_v^T \\ q_0 E^{3\times 3} + \boldsymbol{q}_v^{\times} \end{bmatrix} \tag{23}$$

where $\boldsymbol{E}^{3\times 3}$ is the identity matrix, $\boldsymbol{q}_v^{\times}$ is the cross-product operator:

$$\boldsymbol{q}_v^{\times} = \begin{bmatrix} 0 & -q_3 & q_2 \\ q_3 & 0 & -q_1 \\ -q_2 & q_1 & 0 \end{bmatrix} \tag{24}$$

4.1. Expected Attitude Motion

As mentioned previously, the expected attitude of the spacecraft is that the z axis of the spacecraft's body fixed frame points to the space debris. The expected pointing direction can be calculated through the relative position vector as:

$$\hat{\boldsymbol{\imath}}_p = -\frac{\boldsymbol{\rho}}{\|\boldsymbol{\rho}\|} \tag{25}$$

When the attitude of the spacecraft reaches the expected pointing direction, $\hat{\boldsymbol{\imath}}_p$ projected into $\{\mathcal{B}\}$ frame is

$${}^{B}\hat{\boldsymbol{\imath}}_p = [0, 0, 1]^T \tag{26}$$

The pointing requirement does not uniquely define the expected attitude of the spacecraft because the angle rotating along the z axis of the spacecraft is not defined.

This paper proposes to utilize the principle rotation to define the expected attitude of the spacecraft. The angular velocity of the spacecraft should be perpendicular to both the z axis of the spacecraft and the expected pointing direction $\hat{\boldsymbol{\imath}}_p$. In this way the expected rotation of the spacecraft is minimized. The expected angular velocity should satisfy

$$\boldsymbol{\omega}_e \cdot \hat{\boldsymbol{\imath}}_p = 0 \tag{27}$$

$$\boldsymbol{\omega}_e \times \hat{\boldsymbol{\imath}}_p = \dot{\hat{\boldsymbol{\imath}}}_p \tag{28}$$

Taking a cross product of Eq. (28) from left by $\hat{\boldsymbol{\imath}}_p$, yields

$$\begin{aligned} \hat{\boldsymbol{\imath}}_p \times \dot{\hat{\boldsymbol{\imath}}}_p =& \hat{\boldsymbol{\imath}}_p \times (\boldsymbol{\omega}_e \times \hat{\boldsymbol{\imath}}_p) \\ =& \boldsymbol{\omega}_e(\hat{\boldsymbol{\imath}}_p \cdot \hat{\boldsymbol{\imath}}_p) + \hat{\boldsymbol{\imath}}_p(\hat{\boldsymbol{\imath}}_p \cdot \boldsymbol{\omega}_e) = \boldsymbol{\omega}_e \end{aligned} \tag{29}$$

Thus the expression of $\boldsymbol{\omega}_e$ is obtained:

$$\boldsymbol{\omega}_e = \hat{\boldsymbol{\imath}}_p \times \dot{\hat{\boldsymbol{\imath}}}_p \tag{30}$$

Note that $\hat{\boldsymbol{\imath}}$ is defined by Eq. (25). Taking a first order time derivative of Eq. (25), yields

$$\dot{\hat{\boldsymbol{\imath}}}_p = -\frac{\dot{\boldsymbol{\rho}}}{\|\boldsymbol{\rho}\|} + \frac{\boldsymbol{\rho} \cdot \dot{\boldsymbol{\rho}}}{\|\boldsymbol{\rho}\|^3}\boldsymbol{\rho} \tag{31}$$

The expected angular velocity can be expressed as

$$\boldsymbol{\omega}_d = \hat{\boldsymbol{e}}_r \times \dot{\hat{\boldsymbol{e}}}_r \tag{32}$$

unfold pointing direction unit vector in coordinate system $\{\mathcal{N}\}$ and take the derivative of it,yields

$${}^{N}\dot{\hat{\boldsymbol{e}}}_r = \frac{d}{dt}\left(\frac{\boldsymbol{d}}{\|\boldsymbol{d}\|}\right) = \frac{{}^{N}\dot{\boldsymbol{d}}}{\|\boldsymbol{d}\|} + \left[\frac{d}{dt}\frac{1}{\|\boldsymbol{d}\|}\right]{}^{N}\boldsymbol{d} = \left(\boldsymbol{E}_{3\times 3} - {}^{N}\hat{\boldsymbol{e}}_r \cdot {}^{N}\hat{\boldsymbol{e}}_r^T\right)\frac{{}^{N}\dot{\boldsymbol{d}}}{\|\boldsymbol{d}\|} \tag{33}$$

where $\dot{\boldsymbol{d}}$ is velocity of tracking spacecraft relative to space debris.

Take the derivative of Eq. (33),yields

$$\begin{aligned} {}^{N}\ddot{\hat{\boldsymbol{e}}}_r =& \left(\boldsymbol{E}_{3\times 3} - {}^{N}\hat{\boldsymbol{e}}_r \cdot {}^{N}\hat{\boldsymbol{e}}_r^T\right)\left[\frac{{}^{N}\ddot{\boldsymbol{d}}}{\|\boldsymbol{d}\|} - \left({}^{N}\dot{\boldsymbol{d}} \cdot {}^{N}\dot{\boldsymbol{d}}^T\right)\frac{{}^{N}\hat{\boldsymbol{e}}_r}{\|\boldsymbol{d}\|^2}\right] \\ & - \left({}^{N}\dot{\hat{\boldsymbol{e}}}_r \cdot {}^{N}\hat{\boldsymbol{e}}_r^T + {}^{N}\hat{\boldsymbol{e}}_r \cdot {}^{N}\dot{\hat{\boldsymbol{e}}}_r^T\right)\frac{{}^{N}\dot{\boldsymbol{d}}}{\|\boldsymbol{d}\|} \end{aligned} \tag{34}$$

Take the derivative of Eq. (32),yields

$$\dot{\boldsymbol{\omega}}_d = \hat{\boldsymbol{e}}_r \times \ddot{\hat{\boldsymbol{e}}}_r \tag{35}$$

The expected angular velocity and the desired angular acceleration can be calculated by above equations. Then expected quaternion can be computed through integrating the follow equation

$$\dot{\boldsymbol{q}}_d = \frac{1}{2}B(\boldsymbol{q}_d)\,\boldsymbol{\omega}_d \tag{36}$$

4.2. Nonlinear Control

Attitude control of a rigid body has important applications to spacecraft. Various control laws have been developed for pointing and slewing. To enhance the control ability of a spacecraft system, globally stabilizing control laws are designed for attitude control.

Define error quaternions as q_e, it can be determined by follow equation

$$q_e = q_d^{-1} \otimes q = \begin{bmatrix} q_0 & -q_1 & -q_2 & -q_3 \\ q_1 & q_0 & q_3 & -q_2 \\ q_2 & -q_3 & q_0 & q_1 \\ q_3 & q_2 & -q_1 & q_0 \end{bmatrix}\begin{bmatrix} q_{d0} \\ -q_{d1} \\ -q_{d2} \\ -q_{d3} \end{bmatrix} \tag{37}$$

where $q_e = [q_{e0}; \boldsymbol{q}_{ev}]$, with $\boldsymbol{q}_{ev} = [q_{e1}; q_{e2}; q_{e3}]$. When $q_e = [1; 0; 0; 0]$, it it means $q_d = q$, so the attitude target has been achieved.

The angular velocity tracking errors are defined as follows

$$\boldsymbol{\omega}_e = \boldsymbol{\omega} - \boldsymbol{\omega}_d \tag{38}$$

a attitude control law can be designed as

$$\boldsymbol{T}_c = \boldsymbol{\omega} \times \boldsymbol{J}\boldsymbol{\omega} + \boldsymbol{J}\dot{\boldsymbol{\omega}}_d - \boldsymbol{D}\boldsymbol{\omega}_e - \boldsymbol{K}\boldsymbol{q}_{ev} \tag{39}$$

where $\boldsymbol{D}$ and $\boldsymbol{K}$ are diagonal matrix with positive diagonal elements.

Define Lyapunov function as

$$
\begin{aligned}
V_a &= \frac{1}{2}\left(\boldsymbol{K}^{-1}\boldsymbol{\omega}_e\right)^T \boldsymbol{J}\boldsymbol{\omega}_e + \left[\boldsymbol{q}_{ev}^T\boldsymbol{q}_{ev} + (q_{e0}-1)^2\right] \\
&\quad + \varepsilon\left(\boldsymbol{\omega}_e^T\boldsymbol{q}_{ev} - \frac{1}{2}\boldsymbol{\omega}_e^T\boldsymbol{K}_1^{-1}\boldsymbol{D}_1\boldsymbol{\omega}_e\right) \\
&= \frac{1}{2}\left(\boldsymbol{K}^{-1}\boldsymbol{\omega}_e\right)\boldsymbol{J}\boldsymbol{\omega}_e + 2\left(1-q_{e0}\right) \\
&\quad + \varepsilon\left[\boldsymbol{\omega}_e^T\boldsymbol{q}_{ev} - \frac{1}{2}\boldsymbol{\omega}_e^T\boldsymbol{K}_1^{-1}\boldsymbol{D}_1\boldsymbol{\omega}_e\right]
\end{aligned} \tag{40}
$$

where ε is positive scalar constant,

$$\boldsymbol{K}_1 = \boldsymbol{J}^{-1}\boldsymbol{K} \tag{41a}$$

$$\boldsymbol{D}_1 = \boldsymbol{J}^{-1}\boldsymbol{D} \tag{41b}$$

$$\boldsymbol{K}_1^{-1}\boldsymbol{D}_1 = \boldsymbol{K}^{-1}\boldsymbol{D} \tag{41c}$$

Taking the derivative of V_a, yields

$$
\begin{aligned}
\dot{V}_a &= \left(\boldsymbol{K}^{-1}\boldsymbol{\omega}_e^T\right)\left(-\boldsymbol{D}\boldsymbol{\omega}_e - \boldsymbol{K}\boldsymbol{q}_{ev}\right) + \boldsymbol{\omega}_e^T\boldsymbol{q}_{ev} \\
&\quad + \varepsilon\Big[\boldsymbol{q}_{ev}^T\left(-\boldsymbol{D}_1\boldsymbol{\omega}_e - \boldsymbol{K}_1\boldsymbol{q}_{ev}\right) + \frac{1}{2}\boldsymbol{\omega}_e^T\left(q_{e0}\boldsymbol{\omega}_e - \boldsymbol{\omega}_e^{\times}\boldsymbol{q}_{ev}\right) \\
&\quad - \left(\boldsymbol{D}_1\boldsymbol{K}_1^{-1}\boldsymbol{\omega}_e^T\right)\left(-\boldsymbol{D}_1\boldsymbol{\omega}_e - \boldsymbol{K}_1\boldsymbol{q}_{ev}\right)\Big] \\
&= -\boldsymbol{\omega}_e^T\boldsymbol{K}^{-1}\boldsymbol{D}\boldsymbol{\omega}_e - \boldsymbol{\omega}_e^T\boldsymbol{q}_{ev} + \boldsymbol{\omega}_e^T\boldsymbol{q}_{ev} \\
&\quad + \varepsilon\Big(-\boldsymbol{q}_{ev}^T\boldsymbol{D}_1\boldsymbol{\omega}_e - \boldsymbol{q}_{ev}^T\boldsymbol{K}_1\boldsymbol{q}_{ev} + \frac{q_{e0}}{2}\boldsymbol{\omega}_e^T\boldsymbol{\omega}_e \\
&\quad + \boldsymbol{\omega}_e^T\boldsymbol{D}_1^2\boldsymbol{K}_1^{-1}\boldsymbol{\omega}_e + \boldsymbol{\omega}_e^T\boldsymbol{D}_1\boldsymbol{q}_{ev}\Big) \\
&= -\boldsymbol{\omega}_e^T\boldsymbol{K}^{-1}\boldsymbol{D}\boldsymbol{\omega}_e + \varepsilon\Big(-\boldsymbol{q}_{ev}^T\boldsymbol{K}_1\boldsymbol{q}_{ev} + \frac{q_{e0}}{2}\boldsymbol{\omega}_e^T\boldsymbol{\omega}_e \\
&\quad + \boldsymbol{\omega}_e^T\boldsymbol{D}_1^2\boldsymbol{K}_1^{-1}\boldsymbol{\omega}_e\Big) \\
&= -\boldsymbol{\omega}_e^T\boldsymbol{K}^{-1}\boldsymbol{D}\boldsymbol{\omega}_e - \varepsilon\boldsymbol{q}_{ev}^T\boldsymbol{K}_1\boldsymbol{q}_{ev} \\
&\quad + \varepsilon\left[\boldsymbol{\omega}_e^T\left(q_{e0}\boldsymbol{E}_{3\times3} + \boldsymbol{D}_1^2\boldsymbol{K}_1^{-1}\right)\boldsymbol{\omega}_e\right] \\
&= -\boldsymbol{\omega}_e^T\left[\boldsymbol{K}^{-1}\boldsymbol{D} - \varepsilon\left(q_{e0}\boldsymbol{E}_{3\times3} + \boldsymbol{J}^{-1}\boldsymbol{D}\boldsymbol{K}^{-1}\boldsymbol{D}\right)\right]\boldsymbol{\omega}_e \\
&\quad - \varepsilon\boldsymbol{q}_{ev}^T\boldsymbol{K}_1\boldsymbol{q}_{ev}
\end{aligned} \tag{42}
$$

When ε is small enough, V is positive definite function with infinitesimal upper bound, $\dot{V}$ is global negative definite function, so the control law is asymptotically stabilizing. This control law is applicable for attitude control with large initial error, so it is useful for both small-range attitude stability and wide-range attitude maneuver.

5. Numerical Simulations

The scope and effect of the previous control law will be analyzed through numerical simulations of several typical states of space debris's motion. The initial orbit parameters of tracking spacecraft and space debris are described by six Keplerian elements. The initial position error is $14.2m$ and the initial velocity error is $8.87896m/s$. Those initial parameters apply to all conditions of space debris. The following table gives initial six Keplerian elements of tracking spacecraft and space debris.

Gravitational parameter $\mu = 398601km^3/s^2$, mean molar quantity radius of the earth is $6378.137km$, mass of tracking spacecraft $m_d = 50kg$. The expected distance $l_e = 5m$. Numerical simulations of several typical states of space debris's motion will be analyzed, positive definite 3×3 position feedback gain matrix $[K_1] = 0.02E_{3\times3}$, $[K_2] = 0.02E_{3\times3}$. Tracking spacecraft's moment of inertia are $[3,3,5]km/m^2$ relative to tracking spacecraft body coordinate system B_d, initial Euler angle are $[60°, 60°, 60°]$, initial angle velocity are $[0,0,0]$ in body coordinate system B_d of the tracking spacecraft. As for attitude control, feedback gain matrix $[K] = E_{3\times3}$, $[D] = 3E_{3\times3}$.

Table 1. initial Orbit elements of tracking spacecraft and space debris

	$a(km)$	$i(°)$	$\Omega(°)$	e	$\omega(°)$	$\theta(°)$
debris	7978.14	55	0	0	113.6	306.4
spacecraft	7978.14	55	0	0	144.979	275.02

5.1. Tracking control of space debris in precession

The objective of tracking spacecraft is keep the tracking spacecraft's barycenter stay $5m$ above the Z axis in body coordinate system B of the space debris, space debris is uncontrolled in this paper. Initial parameters of spinning space debris are shown in Tab. 2 (moment of inertia's unit is in $kg\cdot m^2$, Euler angles' unit are in degree, angular velocity's unit is in rad/s)

Table 2. attitude parameter of space debris in precession

I_x	I_y	I_z	ϕ	θ	ψ	ω_x	ω_y	ω_z
500	500	1000	0	0	0	0	0.1π	0.4π

Tracking simulation of tracking spacecraft relative to space debris in precession are shown in Fig. 3-10.

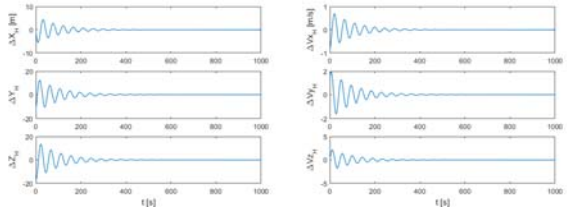

Fig. 3. Position and velocity errors.

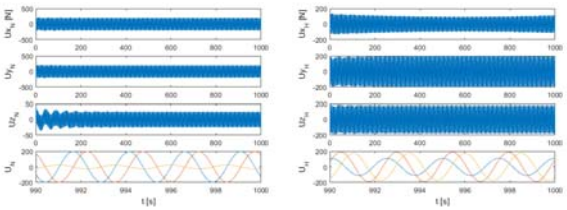

Fig. 4. Control force and component.

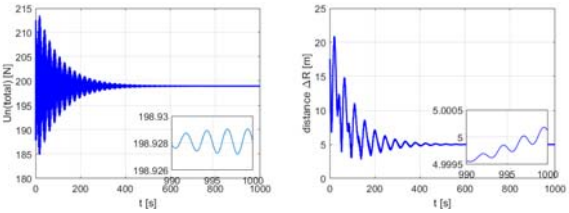

Fig. 5. Control force and distance error.

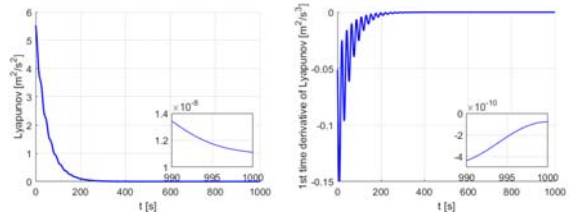

Fig. 6. Lyapunov function and its derivative.

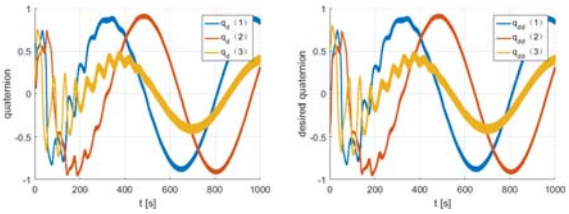

Fig. 7. Tracking spacecraft quaternion and desired quaternion.

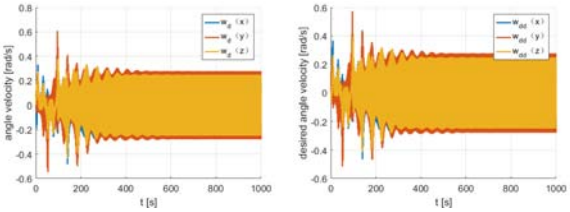

Fig. 8. Tracking spacecraft angle velocity and desired angle velocity.

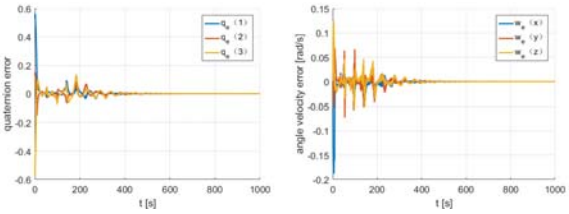

Fig. 9. Quaternion errors and angle velocity errors.

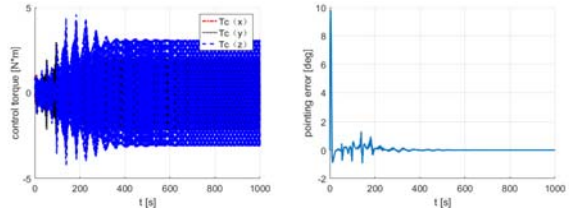

Fig. 10. Control torque and pointing error.

Fig. 3 shows the time histories of position and velocity errors in coordinate system $\{\mathcal{N}\}$, and Fig. 9 shows the time histories of quaternion errors and angle velocity errors. It is seen that under the control force and torques as shown in Fig. 5 and Fig. 10, both the position and velocity tracking errors and the attitude errors converge rapidly and satisfy the accuracy requirements despite the situation of the space debris in precession.

5.2. Tracking control of tumbling space debris

Initial parameters of rolling space debris are shown in Tab. 3(moment of inertia's unit is in $kg \cdot m^2$, Euler angles' unit are in degree, angular velocity's unit is in rad/s)

Table 3. attitude parameter of rolling space debris

I_x	I_y	I_z	ϕ	θ	ψ	ω_x	ω_y	ω_z
500	700	1000	0	0	0	0	0.2π	0.01π

Simulation of tracking spacecraft relative to rolling space debris are shown in Fig. 11-18.

Fig. 11 shows the time histories of position and velocity errors in coordinate system $\{\mathcal{N}\}$, and Fig. 17 shows the time histories of quaternion errors and angle velocity errors. It is seen that under the control force and torques as shown in Fig. 13 and Fig. 18, both the position and velocity tracking errors and the attitude errors converge rapidly and satisfy the accuracy requirements despite the situation of the rolling space debris.

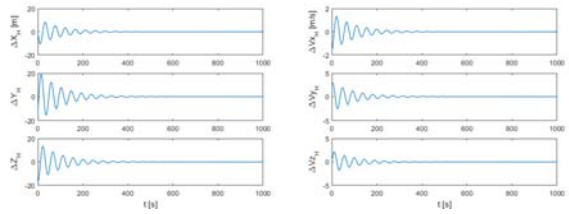

Fig. 11. Position and velocity errors.

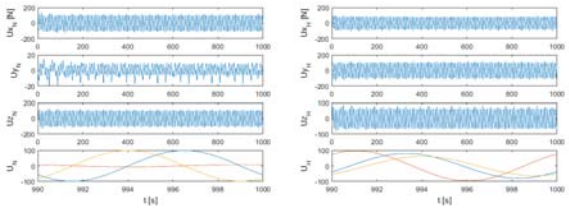

Fig. 12. Control force and component.

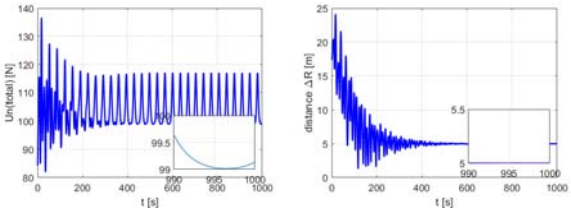

Fig. 13. Control force and distance between tracking spacecraft and space debris.

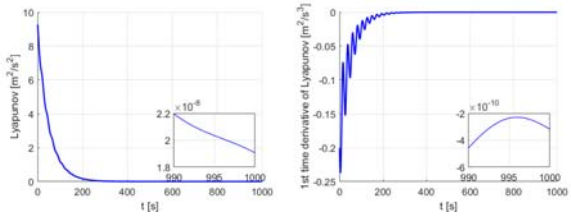

Fig. 14. Lyapunov function and its derivative.

6. Conclusion

In this paper, a close-proximity tracking of a space debris problem is investigated. A highly coupled control is developed to fulfill the tracking problem. The expected location and attitude of the tracking spacecraft is resolved and a nonlinear control law based on Lyapunov function is developed. with the awareness of the singularity rejection, a potential function control method to avoid the singularity is designed. A numerical simulation of two situations was presented to illustrate the efficacy of this control design.

Acknowledgement

This research was supported by the National Natural Science Foundation of China No. 11672294.

References

1) J. A. Borja and D. Tun, "Deorbit Process Using Solar Radiation Force," *Journal of Spacecraft and Rockets*, Vol. 43, No. 3, 2006, pp. 685–687.
2) S. I. Nishida, S. Kawamoto, and Y. Okawa, "Space debris removal system using a small satellite," *Acta Astronautica*, Vol. 65, July-August 2009, pp. 95–102.
3) L. Visagie and T. Theodorou, "Hybrid solar sails for active deorbit removal," Standard 10-6411b, ESA, Paris, June 2011.

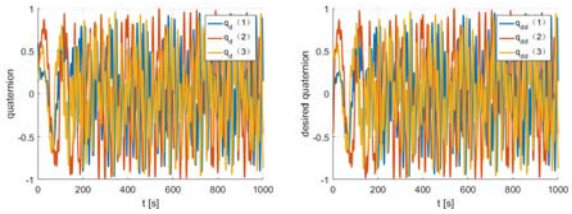

Fig. 15. Tracking spacecraft quaternion and desired quaternion.

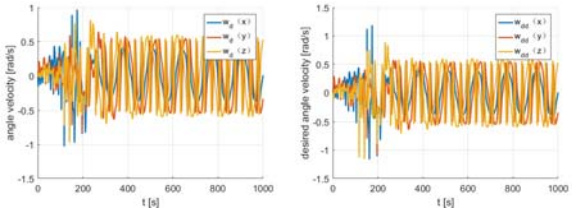

Fig. 16. Tracking spacecraft angle velocity and desired angle velocity.

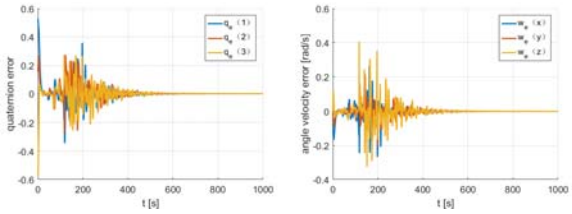

Fig. 17. Quaternion errors and angle velocity errors.

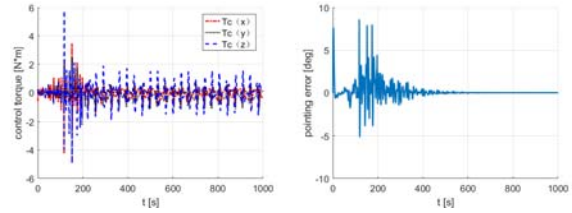

Fig. 18. Control torque and pointing error.

4) T. Schildknecht, "Optical surveys for space debris," *The Astronomy and Astrophysics Review*, Vol. 14, No. 1, 2007, pp. 44–111.
5) L. T. DeLuca, F. Bernelli, F. Maggi, and P. Tadini, "Active space debris removal by a hybrid propulsion module," *Acta Astronautica*, Vol. 91, 2013, pp. 20–33.
6) S. I. Nishida and S. Kawamoto, "Strategy for capturing of a tumbling space debris," *Acta Astronautica*, Vol. 68, No. 1, 2011, pp. 113–120.
7) F. B. Estabrook and H. D. Wahlquist, "Response of Doppler spacecraft tracking to gravitational radiation," *General Relativity and Gravitation*, Vol. 6, October 1975, pp. 439–447.
8) M. D. Queiroz, V. Kapila, and Q. G. Yan, "Adaptive Nonlinear Control of Multiple Spacecraft Formation Flying," *Journal of Guidance Control and Dynamics*, Vol. 23, May-June 2000, pp. 385–390.
9) B. J. Naasz, C. D. Hall, and C. D. Karlgaard, "Application of several control techniques for the ionospheric observation nanosatellite formation," *Advances in the Astronautical Sciences*, Vol. 112, No. 2, 2002, pp. 1063–1079.
10) D. Lee and G. Vukovich, "Adaptive finite-time control for spacecraft hovering over an asteroid," *IEEE Transactions on Aerospace and Electronic Systems*, Vol. 52, No. 3, 2016, pp. 1183–1196.
11) Y. Rao, J. Yin, and C. Han, "Hovering Formation Design and Control Based on Relative Orbit Elements," *Journal of Guidance, Control, and Dynamics*, Vol. 39, No. 2, 2015, pp. 360–371.
12) M. W. Thein, J. Thienel, R. Luquette, and D. Tsai, "Relative Position Estimation and Control for Precision Formation Flying of Two Spacecraft Formations," *AIAA Guidance, Navigation and Control Conference and Exhibit*, August 2007, p. 6754.
13) M. Ramp and E. Papadopoulos, "Attitude and Angular Velocity Tracking for a Rigid Body using Geometric Methods on the Two-Sphere," *In Control Conference (ECC)*, European, IEEE, July 2015, pp. 3238–3243.
14) K. Subbarao and M. R. Akella, "Differentiator-Free Nonlinear Proportional-Integral Controllers for Rigid-Body Attitude Stabilization," *Journal of Guidance, Control, and Dynamics*, Vol. 27, No. 6, 2004, pp. 1092–1096.
15) S. Li, S. Ding, and Q. Li, "Global set stabilization of the spacecraft attitude control problem based on quaternion," *International Journal of Robust and Nonlinear Control*, Vol. 20, No. 1, 2010, pp. 84–105.
16) J. Su and K. Y. Cai, "Globally Stabilizing Proportional-Integral-Derivative Control Laws for Rigid-Body Attitude Tracking," *Journal of Guidance, Control, and Dynamics*, Vol. 34, No. 4, 2011, pp. 1260–1264.
17) R. Wisniewski, "Linear Time-Varying Approach to Satellite Attitude Control Using Only Electromagnetic Actuation," *Journal of Guidance, Control, and Dynamics*, Vol. 23, No. 4, 2000, pp. 640–647.
18) B. Xiao, Q. Hu, and Y. Zhang, "Adaptive Sliding Mode Fault Tolerant Attitude Tracking Control for Flexible Spacecraft Under Actuator Saturation," *IEEE Transactions on Control Systems Technology*, Vol. 20, No. 6, 2012, pp. 1605–1612.
19) A. M. Zou, K. K. D., Z. G. Hou, and X. Liu, "Finite-Time Attitude Tracking Control for Spacecraft Using Terminal Sliding Mode and Chebyshev Neural Network," *IEEE Transactions on Systems, Man, and Cybernetics, Part B (Cybernetics)*, Vol. 41, No. 4, 2011, pp. 950–963.
20) G. Q. Xing and S. A. Parvez, "Nonlinear Attitude State Tracking Control for Spacecraft," *Journal of Guidance, Control, and Dynamics*, Vol. 24, No. 3, 2001, pp. 624–626.
21) W. Luo, Y. C. Chu, and K. V. Ling, "Inverse optimal adaptive control for attitude tracking of spacecraft," *IEEE Transactions on Automatic Control*, Vol. 50, No. 11, 2005, pp. 1639–1654.
22) H. Pan and V. Kapila, "Adaptive nonlinear control for spacecraft formation flying with coupled translational and attitude dynamics," *in Proc. of the conf. on IEEE, Decision and Control*, Vol. 3 of *In*, 2001, pp. 2057–2062.
23) H. Pan, "Integrated nonlinear optimal control of spacecraft in proximity operations," *International Journal of Control*, Vol. 83, No. 2, 2010, pp. 347–363.
24) W. Y. H., C. X. B., and X. Y. J., "Relative motion coupled control for formation flying spacecraft via convex optimization," *Aerospace Science and Technology*, Vol. 14, No. 6, 2010, pp. 415–428.
25) W. J. Y., L. H. Z., and S. Z. W., "Relative motion coupled control based on dual quaternion," *International Journal of Control*, Vol. 25, No. 1, 2013, pp. 102–113.
26) C. M. Pong and D. W. Miller, "Reduced-Attitude Boresight Guidance and Control on Spacecraft for Pointing, Tracking, and Searching," *Journal of Guidance, Control, and Dynamics*, Vol. 38, No. 6, 2015, pp. 1027–1035.
27) D. Lee and H. Pernicka, "Optimal Control for Proximity Operations and Docking," *International Journal Aeronautical and Space Sciences*, Vol. 11, No. 3, 2010, pp. 206–220.
28) W. H. Clohessy and R. S. Wiltshire, "Terminal Guidance System for Satellite Rendezvous," *Journal of Aerospace Sciences*, Vol. 27, September 1960, pp. 653–658.